Aberrant Sensory Innervation of the Olfactory Bulb in Neuropilin-2 Mutant Mice

Walz, Andreas; Rodriguez, Ivan; Mombaerts, Peter

How to cite

WALZ, Andreas, RODRIGUEZ, Ivan, MOMBAERTS, Peter. Aberrant Sensory Innervation of the Olfactory Bulb in Neuropilin-2 Mutant Mice. In: The Journal of neuroscience, 2002, vol. 22, n° 10, p. 4025–4035. doi: 10.1523/JNEUROSCI.22-10-04025.2002

This publication URL: https://archive-ouverte.unige.ch/unige:174958
Publication DOI: 10.1523/JNEUROSCI.22-10-04025.2002

The Journal of Neuroscience, May 15, 2002, 22(10):4025–4035

Aberrant Sensory Innervation of the Olfactory Bulb in Neuropilin-2 Mutant Mice

Andreas Walz, Ivan Rodriguez, and Peter Mombaerts

The Rockefeller University, New York, New York 10021

The mammalian olfactory system consists of two anatomically segregated structures, the main olfactory system and the vomeronasal system, which each detect distinct types of chemical stimuli in the environment. During development, sensory neurons establish precise axonal connections with their respective targets within the olfactory bulb. The specificity of the odorant or vomeronasal receptor expressed by the sensory neuron is crucial in this process, yet it is less clear which of the more conventional axon guidance molecules are involved. Here, we show that neuropilin-2, a coreceptor for some of the class 3 semaphorins, is expressed in subpopulations of olfactory and vomeronasal sensory neurons. We generated a knockout mutation in the neuropilin-2 gene by gene targeting in embryonic stem cells. Neuropilin-2 mutant mice exhibit profound and distinct effects on target innervation within the olfactory bulb. In the main olfactory system, axons of olfactory sensory neurons penetrate into the deeper layers of the main olfactory bulb. In the vomeronasal system, axonal fasciculation within the vomeronasal nerve is affected; some axons are misrouted and innervate glomeruli in an ectopic domain of the accessory olfactory bulb.

Key words: olfaction; smell; odor; olfactory bulb; vomeronasal system; neuropilin; semaphorin; axon guidance

The sense of smell depends on the ability of specialized neurons to interact with and respond to a vast variety of chemicals. In terrestrial mammals, olfactory sensory neurons (OSNs) are located on the turbinates in the caudal aspect of the nasal cavity and project their axons to the main olfactory bulb (MOB). There, OSN axons synapse with second-order neurons (mitral and tufted cells) within specialized compartments of neuropil called glomeruli. OSNs expressing a particular odorant receptor (OR) gene from the available repertoire of ~1000 genes project their axons to a few common glomeruli (Ressler et al., 1994; Vassar et al., 1994; Mombaerts et al., 1996). In many mammalian species, a second olfactory system, the vomeronasal system, is thought to be specialized in the perception of stimuli related to social and reproductive behaviors (Halpern, 1987; Keverne, 1999). The sensory neurons reside within an oblong-shaped structure, the vomeronasal organ (VNO), situated at the rostral end of the nasal cavity. Axons of these vomeronasal sensory neurons (VSNs) project to the accessory olfactory bulb (AOB), a structure that is anatomically distinct from the MOB. Glomeruli also form the targets for VSN axons, but the glomerular structures are less well defined in the AOB compared with the MOB (Meisami and Bhatnagar, 1998). This high degree of specificity of axonal connections poses a formidable task for the developing olfactory system (Mombaerts, 2001).

Several axon guidance molecules have been described to be expressed in both olfactory systems (Treloar et al., 1997; Yoshihara et al., 1997; Pasterkamp et al., 1999; St. John and Key, 2001). Among these are neuropilin-1 (NP1) and neuropilin-2 (NP2), coreceptors for a subfamily of secreted repulsive guidance cues, class 3 semaphorins. NP1 was first identified as a high-affinity receptor for class 3 semaphorins, and the molecular cloning of NP2 helped explain some of the specificity of semaphorin activities (Chen et al., 1997; He and Tessier-Lavigne, 1997; Kolodkin et al., 1997; Giger et al., 1998). It is now thought that homodimers of NP1 bind sema3A, whereas heterodimers of NP1 and NP2 act as sema3C receptors, and homodimers of NP2 alone confer responsiveness to sema3B and sema3F (Chen et al., 1998; Raper, 2000; Zou et al., 2000). Neuropilins, however, do not possess a signal-transducing activity but act together with other transmembrane proteins, plexins, to induce collapsing activity by class 3 semaphorins (Winberg et al., 1998; Takahashi et al., 1999). Neuropilins determine class 3 semaphorin specificity, as evidenced by the profound disruption of axonal pathfinding of several types of NP2-expressing neurons in the absence of NP2 activity (Chen et al., 2000; Giger et al., 2000).

Here, we describe a novel targeted *NP2* mutation in which the axonal marker tau-green fluorescent protein (GFP) is placed under the control of the *NP2* promoter, precluding expression of endogenous NP2. We show that deficiency of NP2 results in improper axonal innervation of the MOB and AOB by OSNs and VSNs, respectively, providing functional evidence for a role of NP2 in axon pathfinding to the olfactory bulb.

MATERIALS AND METHODS

Targeting vector. *NP2*-specific primers at the 5′ end of the coding region were used to generate a probe by reverse transcription (RT)-PCR to screen a 129/SvJ mouse bacterial artificial chromosome genomic library (Genome Systems, St. Louis, MO). The primer sequences used are as follows: forward primer, 5′-ATGGATATGTTTCCTCTTACCTGG-3′; and reverse primer, 5′-GAGTTACTTCAGTATGAACGTCAG-3′. An *Acc*I–*Xba*I fragment containing the 5′ end of the *NP2* gene was subcloned into pBluescript II SK(+) (Stratagene, La Jolla, CA) and was sequenced in its entirety. A *Pac*I site was placed into a *Kpn*I site 992 bp

Received Dec. 11, 2001; revised Feb. 13, 2002; accepted Feb. 15, 2002.

This work was supported by the National Institutes of Health. We thank H. Nagao and K. Mori (University of Tokyo, Tokyo, Japan) for sharing the NP2 antiserum, J. Miwa and T. Ishii for technical help, and P. Feinstein, J. Miwa, and L. Vosshall for helpful discussion.

Correspondence should be addressed to Peter Mombaerts, The Rockefeller University, 1230 York Avenue, New York, NY 10021. E-mail: peter@rockefeller.edu.

Dr. Rodriguez's present address: Department of Zoology and Animal Biology, University of Geneva, 1211 Geneva 4, Switzerland.

into the first intron, and a *lox*P site 272 bp upstream of the translation start site was inserted by ligation of a *lox*P oligonucleotide into an *Mlu*I site (plasmid NP2–*Pac*I). A *Pme*I site was generated at the 5′ end of the targeting vector for linearization of the construct. A new cassette was designed consisting of *lox*P followed by *tauGFP*, a polyadenylation site (pA^+), and a *pgk-neomycin* expression cassette flanked by *FRT* sites (*FNF*) and was placed into the *Pac*I site of a modified multiple cloning site of pBluescript II SK. The resulting *loxP-tauGFP-pA*$^+$*-FNF* cassette was inserted into NP2–*Pac*I. The version of GFP used was enhanced GFP-1 (Clontech, Palo Alto, CA).

Gene targeting. The targeting vector was linearized with *Pme*I. Electroporation and cell culture of E14 cells (Hooper et al., 1987) were performed as described previously (Mombaerts et al., 1996). Genomic DNA from G418-resistant embryonic stem cell colonies was digested with *Eco*RV and analyzed by Southern blot hybridization with a 3′ probe external to the targeting vector. Germ line transmission was obtained for the NP2 mutation (clone NP2-flox-neo). The *neo*-selectable marker was removed from the targeted mutations by crossing heterozygous mice to *hACTB-Flp* transgenic mice (Dymecki, 1996). Next, deletion of exon 1 and the first part of intron 1 was achieved by crossing mice heterozygous for the NP2-flox-neo allele to *EIIa-Cre* transgenic mice (Lakso et al., 1996). Intercrossing of heterozygous NP2-Δ mice resulted in heterozygous and homozygous NP2-Δ mice that are devoid of the *Cre* and *flp* transgenes. Analysis was performed on mice that did not carry either transgene. Mice were in a mixed (129 × C57BL/6) background and showed 100% penetrance of the olfactory phenotypes described.

Sections and immunohistochemistry. Mice were deeply anesthetized and intracardially perfused with 4% paraformaldehyde, pH 7.4, and post-fixed on ice for 3 hr. They were then frozen in OCT compound (Sakura Finetek, Torrance, CA), and 20 μm sections were cut on a cryostat. Alternatively, fixed brains were cryoprotected in 30% sucrose and 1% paraformaldehyde and sectioned on a sliding microtome. For $G_{i2\alpha}$ staining, primary antibodies (Wako Pure Chemical Industries) were used at a 1:300 dilution, followed by a goat anti-rabbit IgG coupled to Texas Red (Jackson ImmunoResearch, West Grove, PA). For $G_{o\alpha}$ immunostaining, primary antibodies (Medical and Biological Laboratories Co.) were used at a 1:500 dilution, followed by the same secondary antibody. For lacZ immunostaining, primary antibodies (Cappel, Durham, NC) were used at a 1:500 dilution, followed by the same secondary antibody. For lacZ histochemistry, sections were treated as described previously (Mombaerts et al., 1996) and counterstained with a 1% solution of neutral red in PBS (Sigma, St. Louis, MO).

LacZ and GFP expression and quantification. For taulacZ whole-mount analysis, tissues were processed as described previously (Mombaerts et al., 1996), except that the fixation was performed on ice for 10 min. We note that the VR_i2 gene (Rodriguez et al., 1999) has been renamed *V1rb2* (Del Punta et al., 2000). For tauGFP whole mounts, mice were killed by CO_2 asphyxiation, and the olfactory bulb was exposed. 5-bromo-4-chloro-3-indolyl-β-D-galactoside (X-gal)-stained whole-mount specimens were examined with a Zeiss (Thornwood, NY) SV11 stereomicroscope, and sections were examined with a Zeiss Axioplan 2 microscope; images were taken with a Zeiss AxioCam CCD camera. GFP whole mounts, sections, and immunostained sections were examined with a Zeiss LSM 510 confocal microscope. Image files were processed with Adobe Photoshop 6.0, and surface measurements to quantify the area of tauGFP expression in the AOB were performed in Canvas 6.0.

RT-PCR and in situ *hybridization.* RT-PCR was performed with total RNA isolated from freshly dissected VNO, main olfactory epithelium, or complete olfactory bulb. cDNA was generated using oligo(dT) primers from the SuperScript kit (Invitrogen, Rockville, MD). Specific primers for NP2 splice variants and for the first three exons of the open reading frame (ORF) were designed using publicly available sequence information. The resulting PCR products for the splice variants were then subcloned into pGEM-Teasy vector (Promega, Madison, WI) and sequenced from both ends to verify their identity.

DNA fragments spanning the first 800 bp of the *sema3B*, *sema3C*, and *sema3F* ORFs were amplified by RT-PCR from mouse olfactory bulb total RNA and were used as templates to synthesize probes. Specific oligonucleotides were designed from publicly available sequence information. Digoxigenin-labeled probes were prepared by a DIG RNA-labeling kit (Roche Molecular Biochemicals, Indianapolis, IN). Three- to 5-week-old mice were killed by CO_2 asphyxiation, and their brains were removed for embedding in OCT. Coronal or sagittal sections were cut on a cryostat at 20 μm thickness. The procedures used for hybridization, washings, antibody reaction, and color reaction were performed as described previously (Hirota et al., 1992). Images were taken on a Zeiss Axioplan 2 microscope connected to a Zeiss AxioCam CCD camera. Image files were processed with Adobe Photoshop 6.0. With the exception of minor adjustments in brightness and contrast, the images were not altered.

RESULTS

Genomic structure and targeted disruption of *NP2*

The mouse *NP2* gene consists of 18 exons spanning ~108 kb on chromosome *1c2* (Fig. 1*A*). The exon–intron structure is similar to that of the human gene (Rossignol et al., 2000) and features several alternatively spliced exons at the 3′ end (Fig. 1*C*). These splice variants result in proteins with different transmembrane and cytoplasmic domains and have been described in the mouse before (Chen et al., 1997). To identify the particular splice variants present in the olfactory system, RT-PCR was performed with specific primers for NP2a and NP2b isoforms, respectively, using cDNA prepared from either main olfactory or VNO epithelium. Both epithelia express the same three of the possible six variants, indicating that OSNs and VSNs use the same NP2 isoforms (Fig. 1*E*).

A targeted mutation of the *NP2* locus was created by homologous recombination in embryonic stem cells using a combined *Cre-loxP; flp-FRT* approach. The axonal marker tauGFP (Rodriguez et al., 1999), preceded by a *loxP* sequence and followed by a polyadenylation site and a neomycin expression (*pgk-neo*) cassette flanked by *FRT* sites, was placed 1 kb into the first intron. An upstream *loxP* site was inserted 270 bp 5′ of the translational start site (Fig. 1*B*). The resulting mutant allele, *NP2-flox-neo*, was crossed to a mouse line carrying a ubiquitously expressed *flp*-recombinase transgene to remove the *pgk-neo* expression cassette. Subsequently, the first exon corresponding to the first 24 amino acids encompassing the complete signal sequence of NP2 can be removed by crossing to a mouse line carrying a *Cre*-recombinase transgene expressed either from a ubiquitous (as is the case here) or from a specific promoter. The final recombined allele, *NP2*-Δ, thus encodes an mRNA lacking half of the first exon of *NP2* (Fig. 1*B*), greatly reducing, if not precluding, the ability of the mutant NP2 to be targeted to the plasma membrane. The loss of the coding sequence encoding the signal peptide in the *NP2* mRNA was verified by RT-PCR (Fig. 1*D*). In addition, Cre recombination brings the axonal marker tauGFP under the control of the *NP2* promoter. Because tauGFP is followed by a polyadenylation site, the chances of the formation of a functional NP2 protein are further reduced drastically. Consistent with a null phenotype, no NP2 protein could be detected in immunostained sections of homozygous NP2-Δ brains (data not shown).

Heterozygous NP2-Δ mice were intercrossed, and their offspring were examined in a mixed (129 × C57BL/6) genetic background. Homozygous pups are born alive and indistinguishable from their heterozygous and wild-type littermates. Genotypic analysis reveals, however, that homozygous NP2-Δ pups are obtained less frequently (10.9% homozygous, 27.3% wild-type, and 61.8% heterozygous; $n = 165$), but no increased mortality is observed in juveniles and adults. Homozygous NP2-Δ mice often are not able to reproduce. Another striking phenotype in NP2-Δ mice consists of dramatically slowed growth of homozygous pups. A reduction of overall body size is apparent after 2–3 d and results in mice of approximately one-half the normal size at 3 weeks of age. On weaning, homozygous mice catch up with their littermates in body size and are indistinguishable from their

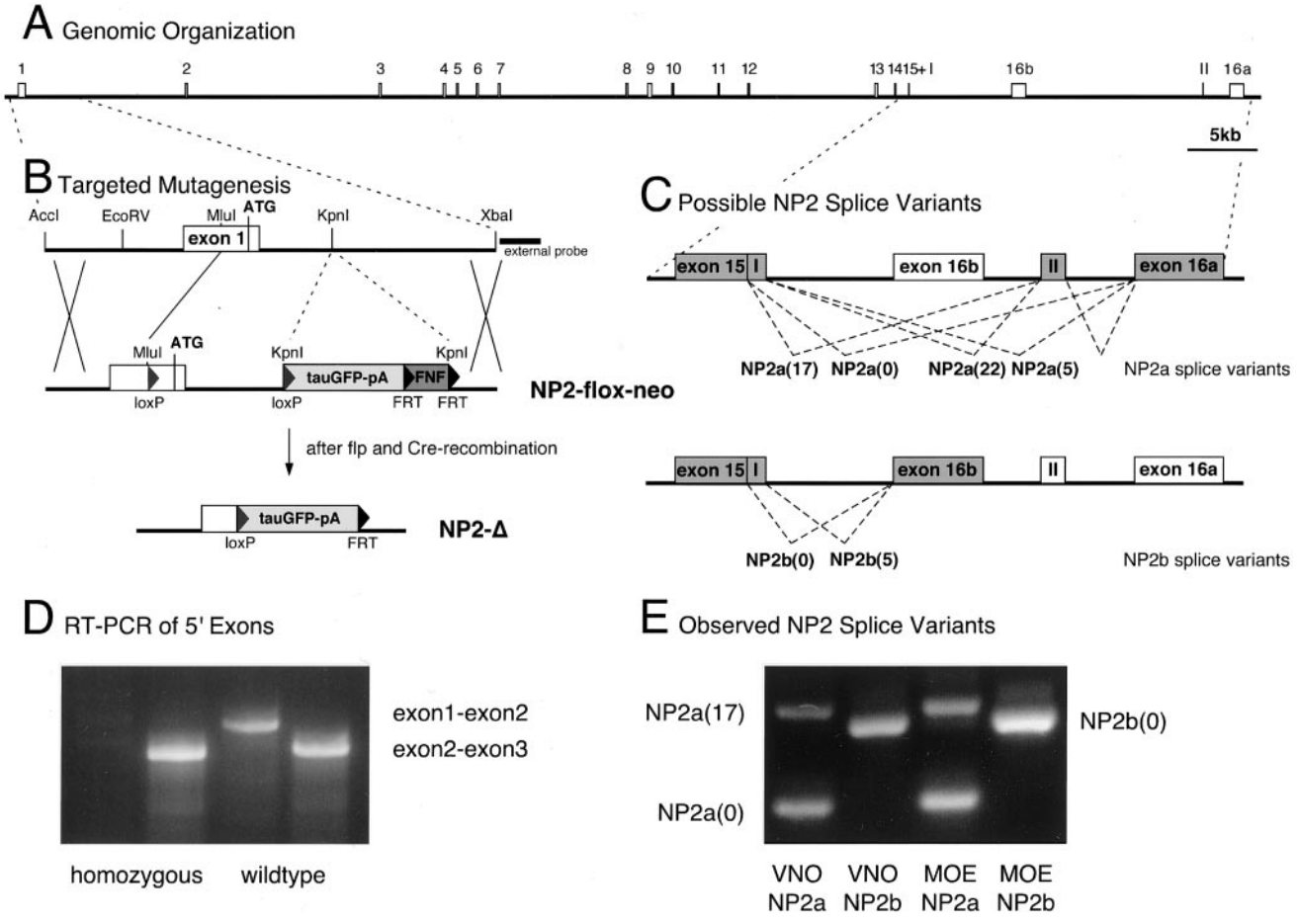

Figure 1. Genomic organization and targeted mutagenesis of the *NP2* locus in mouse. *A*, Exon–intron structure of the *NP2* locus on mouse chromosome *1c2* according to the Celera database. The coding region is spread over 18 exons with alternatively spliced exons 16a, 16b, I, and II at the 3′ end. No other genes are predicted within the *NP2* locus. *B*, Targeting vector for conditional disruption of *NP2*. A *loxP-tauGFP-pA*$^{+}$*-FNF* cassette is inserted into the *Kpn*I site 1 kb into the first intron. A corresponding *lox*P site is inserted into a *Mlu*I site 270 bp upstream of the start codon (*NP2-flox-neo*). The position of the external probe for Southern blot analysis is indicated. After flp recombination, the *pgk-neo* expression cassette (*FNF*) is removed, and after Cre recombination, part of exon 1 including the start codon is removed, and tauGFP-pA^{+} is placed immediately downstream of the *NP2* promoter (*NP2*-Δ). *C*, Possible NP2 splice variants. Two major isoforms (*NP2a*, *NP2b*) are created by alternative splicing of either exon 16a or exon 16b. In addition, exon 15 contains an internal splice acceptor site to create two isoforms omitting five amino acids from *NP2(5)* to create *NP2(0)*. Finally, exon II coding for an additional 17 amino acids in intron 16 can be added to *NP2a* to yield *NP2a(17)* and *NP2a(22)*, respectively. Because exon II is 3′ to exon 16b, these isoforms are not possible for *NP2b*. *D*, 5′ RT-PCR of wild-type and NP2-Δ homozygous mice. cDNA prepared from NP2-Δ homozygous (*lanes 1, 2*) and wild-type (*lanes 3, 4*) mice was used to amplify PCR products spanning exon 1 to exon 2 (*lanes 1, 3*) and exon 2 to exon 3 (*lanes 2, 4*). No product is detectable in *lane 1*, indicating that, as expected, NP2 mRNA from NP2-Δ homozygous mice does not contain the first exon of NP2. *E*, RT-PCR of NP2 splice variants from VNO and main olfactory epithelium (*MOE*) shows that of six possible isoforms, both epithelia express only *NP2a(0)*, *NP2a(17)*, and *NP2b(0)*, indicating that splicing at exon–intron boundary 15 occurs exclusively at the internal splice acceptor site.

siblings after 6–8 weeks. Finally, hydrocephalus is often seen in homozygous but never in heterozygous NP2-Δ mice (63.6%; n = 11; compared with 0%; n = 27). Together, the NP2-Δ allele produces a mutant phenotype similar to another targeted NP2 mutation (Giger et al., 2000).

Neuronal NP2 expression

In heterozygous NP2-Δ mice, axonal projections of NP2-expressing neurons can be visualized as a result of the expression of tauGFP from the mutant allele; the other allele produces NP2 but not tauGFP. In the CNS, tauGFP-positive cells are found in areas previously reported to express NP2 (Chen et al., 1997; Giger et al., 1998, 2000; Chen et al., 2000). Outside the olfactory system, these include the Purkinje cells of the cerebellum, cells inside the deep cerebellar nuclei and several other brainstem nuclei, the hippocampal formation (Fig. 2*A*), and non-neuronal cells such as the lining of blood vessels and the choroid plexus of the fourth ventricle (data not shown). In the olfactory system, cells in the anterior olfactory nucleus (Fig. 2*B*) and piriform cortex (data not shown) express tauGFP. In the peripheral olfactory system, a subset of OSNs express tauGFP in graded patterns from a high lateral level (Fig. 2*C*) to lower medial levels (Fig. 2*D,E*), as has been described for NP2 before (Norlin et al., 2001). TauGFP is also detected in VSNs of the apical ($G_{i2\alpha}$-expressing) layer of the VNO (Fig. 2*F*). Mitral and tufted cells in the AOB (see Fig. 6*A,B*) and early in development also in the MOB (data not shown) are tauGFP-positive.

Axonal projections of OSNs

Next, we determined whether the loss of NP2 has any effect on the sensory projections to the MOB and AOB. OSNs project their axons through the cribriform plate to the MOB, coursing within the outer nerve layer until they reach their target glomeruli (Mombaerts et al., 1996). NP2-positive axons form a set of

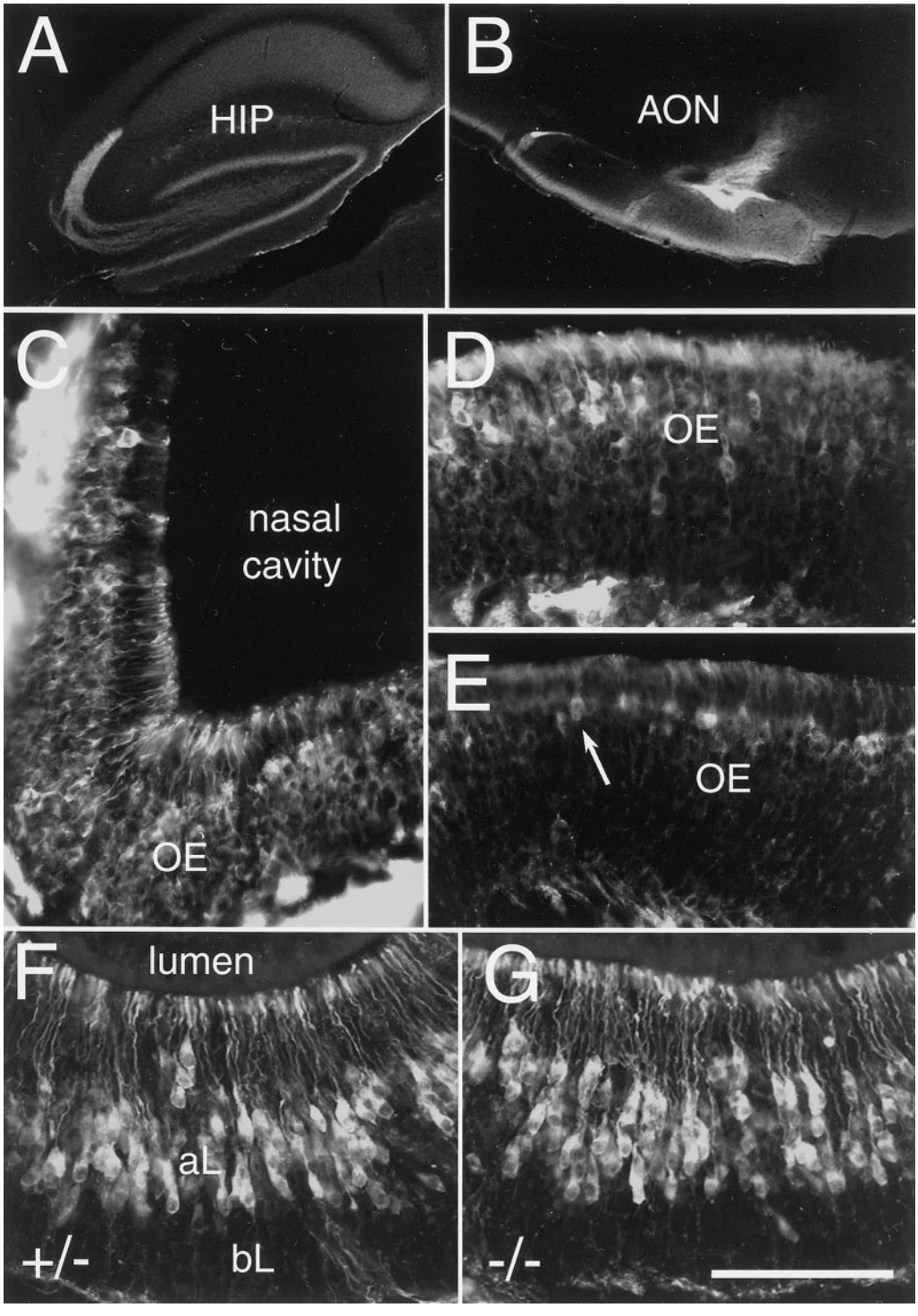

Figure 2. NP2-expressing and NP2-deficient brain areas in heterozygous and homozygous mice. *A, B*, Several areas in the brain positive for tauGFP, including the dentate gyrus in the hippocampus (*HIP*) and the anterior olfactory nucleus (*AON*). *C*, Sixty micrometer coronal section through the main olfactory epithelium (*OE*) of a P21 heterozygous NP2-Δ mouse. Strongly tauGFP-expressing OSNs are located throughout the lateral epithelium and extend dendrites ending in knobs within the nasal cavity. *D*, Intermediate area of the OE with a boundary between an area with greater numbers of tauGFP-expressing OSNs (*left*) and an area of fewer tauGFP-expressing OSNs (*right*). Additionally, OSNs on the *right* express tauGFP at lower levels compared with OSNs on the *left*. *E*, Medial area of the OE with sparse presence of tauGFP-expressing OSNs. Single tauGFP-positive cells can be seen (*arrow*) among many tauGFP-negative cells. *F*, Twenty micrometer coronal section through the VNO of a heterozygous NP2-Δ mouse (+/−). TauGFP-expressing VSNs are located in the apical layer (*aL*) and extend dendrites ending in knobs at the luminal surface. No tauGFP-positive cell bodies are present in the basal layer (*bL*). *G*, Twenty micrometer coronal section through the VNO of a homozygous NP2-Δ mouse (−/−). No gross changes in zonal distribution are detected. Medial is at *top*. Scale bar: *A, B*, 1000 μm; *C–G*, 200 μm.

glomeruli located in two ventral areas, the most anterior tip of the bulb and more prominently in the posterior part close to the border to the telencephalon (Fig. 3*A,B*). This distribution of tauGFP-positive glomeruli is not grossly changed in homozygous NP2-Δ mice compared with heterozygous mice. However, individual OSN axons overshoot their glomerular target and extend into the external plexiform layer (Fig. 3*C*). These axons are only seen in proximity to tauGFP-positive glomeruli and are more abundant in the lateral MOB (Fig. 3*D*). They rarely penetrate the mitral cell layer and are not observed in heterozygous mice (Fig. 3*B*). To confirm that the tauGFP-positive fibers within the external plexiform layer are OSN axons, we crossed NP2 mutant mice to OMP-taulacZ mutant mice, in which all mature OSNs express taulacZ (Mombaerts et al., 1996). Labeling of tauGFP-expressing axons inside the external plexiform layer with an anti-β-galactosidase antibody confirmed that most green fluorescent axons also express taulacZ, indicating that they are misguided OSN axons (Fig. 3*E,F*, *small arrows*). Interestingly, a minority of tauGFP-expressing axons do not label with the anti-β-galactosidase antibody (Fig. 3*E,F*, *large arrows*). It is not clear

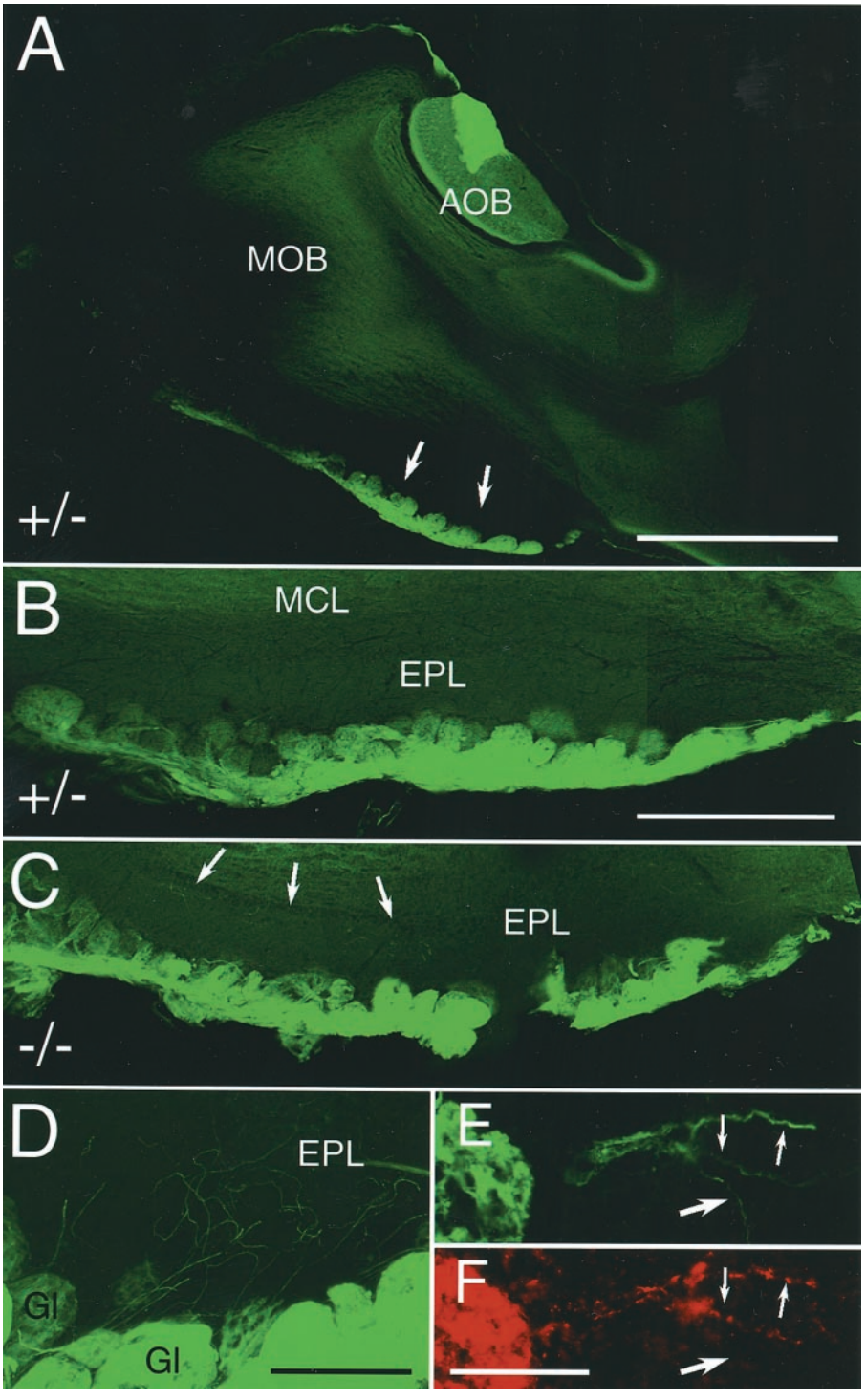

Figure 3. NP2-positive axonal innervation of the ventral MOB in heterozygous and homozygous mice. *A*, Sixty micrometer sagittal sections through the main olfactory bulb (*MOB*) and accessory olfactory bulb (*AOB*) of a P27 heterozygous NP2-Δ mouse (+/−). TauGFP-positive glomeruli are indicated by *arrows*. *B*, Sixty micrometer sagittal section through the ventral MOB of a P35 heterozygous NP2-Δ mouse. Glomeruli innervated by tauGFP-positive OSNs are mainly located at the posterior end of the MOB (to the *right*). No tauGFP-positive fibers are visible in the external plexiform layer (*EPL*) or mitral cell layer (*MCL*). *C*, Sixty micrometer sagittal section through the ventral MOB of a P35 homozygous NP2-Δ mouse (−/−). TauGFP-positive glomeruli appear approximately in the same area as in heterozygous mice. *Arrows* indicate tauGFP-positive fibers extending into the EPL. *D*, Higher magnification of ventral glomeruli in the lateral MOB of a homozygous NP2-Δ mouse. TauGFP-positive axons protrude from tauGFP-positive glomeruli (*Gl*) into the external plexiform layer. *E*, Higher magnification of a glomerulus located ventroanteriorly in the MOB (*left*). Three individual tauGFP-positive axons protrude into the EPL (*small, large arrows*). *F*, Same section as in *E* and immunolabeled for β-galactosidase. Two of the three axons emitting GFP fluorescence are also labeled with anti-β-galactosidase antibodies (*small arrows*), whereas one tauGFP-positive axon is not labeled (*large arrow*). Dorsal is at *top*; anterior to the *left*. Scale bar *A*, 1000 μm; *B, C*, 500 μm; *D*, 200 μm; *E, F*, 50 μm.

whether these axons represent axons of OMP-negative OSNs or whether limited penetration of antibody into the tissue is responsible for the lack of labeling of these axons. No taulacZ-positive, tauGFP-negative fibers are seen within the external plexiform layer, likely reflecting a cell-autonomous effect of the loss of NP2 on axon guidance.

A second set of tauGFP-positive glomeruli are found in the caudal region of the dorsal MOB (see Fig. 5*B*). They are identifiable by their anatomical appearance as belonging to the specialized groups called the modified glomerular complex and the necklace glomeruli, respectively (see Fig. 5*A*). Sensory neurons innervating these glomeruli are biochemically distinct from other OSNs by using cGMP instead of cAMP in their odorant signal transduction cascade (Juilfs et al., 1997) and are thought to be involved in suckling behavior (Greer et al., 1982). Necklace glomeruli are named for their appearance forming a ring of glomeruli surrounding the AOB that are connected by sensory axons like pearls on a string, whereas the modified glomerular complex is formed just anteriorly as a group of two or three medial, closely joined glomeruli (see Fig. 5*A*). In contrast to other NP2-expressing glomeruli in the MOB, the positions of the modified glomerular complex and the necklace glomeruli are shifted

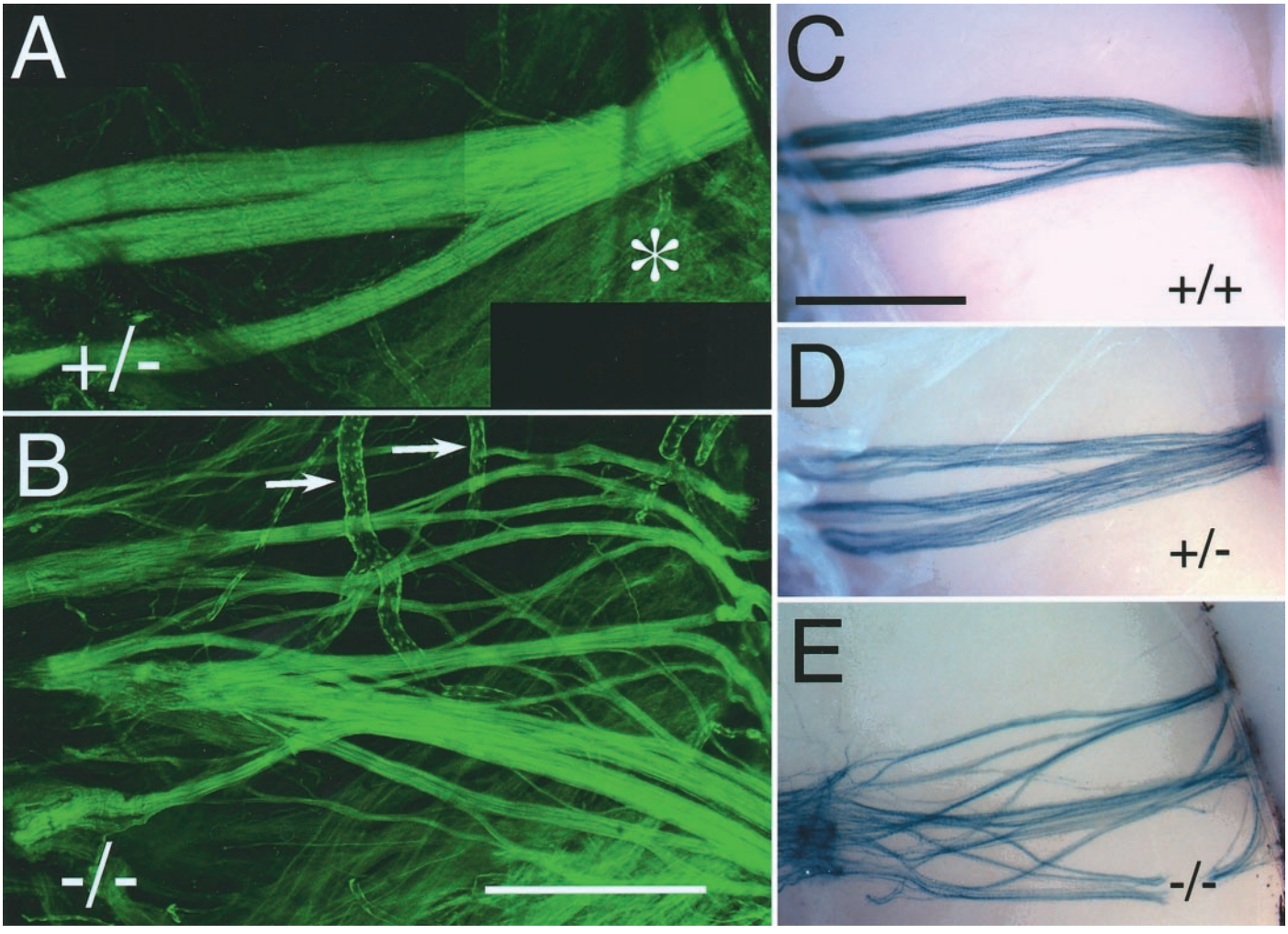

Figure 4. Defasciculation of the vomeronasal nerve in NP2-deficient mice: whole-mount view of the medial surface of the MOB. *A*, GFP fluorescence of VSN axon tracts from the apical layer of the VNO in a P49 heterozygous NP2-Δ mouse (+/−). They penetrate the cribriform plate (*left*) and form tightly fasciculated bundles traversing over the surface of the MOB in a straight trajectory to reach the AOB (*right*). Weaker fluorescence in the ventral part (*asterisk*) corresponds to NP2-positive innervation of the ventral MOB. *B*, VSN axons crossing the surface of the MOB in a P49 homozygous NP2-Δ mouse (−/−). TauGFP-positive axons are much less fasciculated and are spread over a greater area. Ultimately these axon tracts reach the posterior part of the MOB (*right*), but they arrive at unusual angles. Other areas of GFP fluorescence are found in the lining of blood vessels (*arrows*). *C–E*, V1rb2-expressing VSN projections across the MOB in various NP2 backgrounds, as visualized by X-gal staining. Normal fasciculation and trajectories are seen in wild-type (+/+) and heterozygous (+/−) mice. In homozygous (−/−) mice, V1rb2-positive axons are much less fasciculated and take a broader approach to the AOB. Dorsal is at *top*; anterior to the *left*. Scale bars, 500 μm.

along the mediolateral axis in homozygous NP2-Δ mice, and sensory innervation of these glomeruli appears to be somewhat diminished (see Fig. 5*C,D*). The number of glomeruli in these two substructures usually remains the same.

Axonal projections of VSNs

Sensory neurons in the VNO can be subdivided into two distinct groups depending on the location of their cell body in the apical or basal layer of the epithelium. Neurons with cell bodies situated in the apical layer express a distinct class of vomeronasal receptors, the V1rs (Dulac and Axel, 1995). Furthermore, they can be distinguished by their expression of the G-protein subunit $G_{i2\alpha}$ versus $G_{o\alpha}$, which is expressed by neurons in the basal layer (Jia and Halpern, 1996). Only sensory neurons of the apical layer express NP2, as revealed by tauGFP expression in heterozygous NP2-Δ mice (Fig. 2*F*). Axon fascicles emanating from the apical layer of the VNO follow several parallel tracts along the septum to reach the olfactory bulb. After penetrating the cribriform plate, axons in heterozygous NP2-Δ mice form two or three tightly fasciculated bundles that migrate across the medial surface of the MOB on a straight trajectory toward the AOB, which is located caudally to the MOB (Fig. 4*A*). Hence tauGFP-positive VSN axons approach the AOB from the medial aspect of the border between the anterior and posterior halves; once they enter their target area, they turn anteriorly to innervate the anterior AOB exclusively (Figs. 5*B*, 6*A*). Unlabeled axons from the basal, $G_{o\alpha}$-expressing layer of the VNO innervate the posterior half of the AOB (Figs. 5*B*, 6*A*). This innervation pattern, as revealed by tauGFP expression, is apparent from the first postnatal day and is maintained throughout early adult life.

In homozygous NP2-Δ mice, tauGFP-positive axons follow identical tracts through the septum to reach the cribriform plate compared with heterozygous NP2-Δ littermates (data not shown). Across the medial surface of the MOB, however, these axons form many more bundles, which spread over a greater area (Fig.

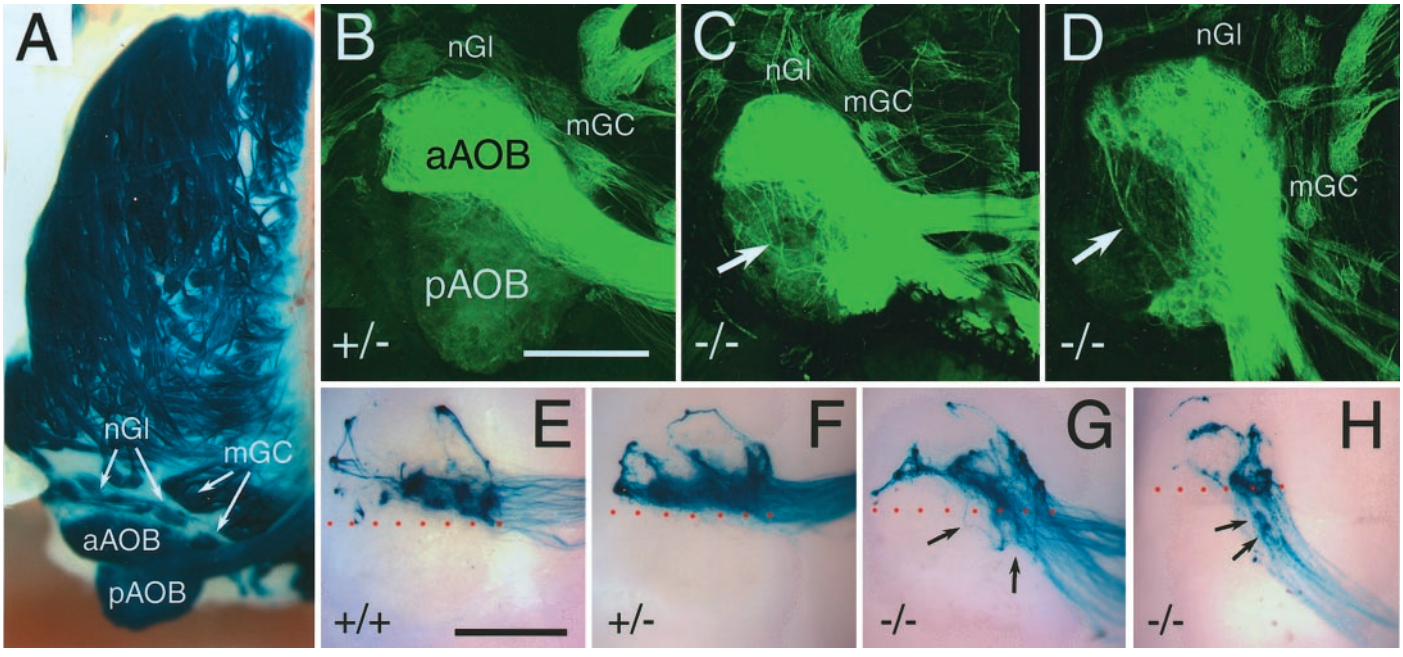

Figure 5. Aberrant sensory innervation of the caudal olfactory bulb. *A*, Whole-mount view of the left dorsal olfactory bulb of an OMP-taulacZ mouse after X-gal staining. The AOB comprises of the anterior (*aAOB*) and posterior (*pAOB*) halves and is located in the caudal region of the olfactory bulb. The necklace glomeruli (*nGl*) form a ring-shaped structure encircling the AOB, whereas the modified glomerular complex (*mGC*) consists of a group of medial, closely joined glomeruli. Anterior is at *top*; medial to the *right*. *B*, GFP fluorescence of NP2-expressing axons of a P34 heterozygous NP2-Δ mouse (+/−). Axon tracts from the apical layer of the VNO arrive medially to innervate the aAOB exclusively. Weak fluorescence in the pAOB is attributable to dendritic staining of tauGFP-positive mitral and tufted cells. In addition, the mGC and the nGl are also tauGFP-positive. *C*, Innervation pattern of the same region in a P34 homozygous NP2-Δ mouse (−/−). VSN axons are now spreading over the medial half of the pAOB in addition to their normal aAOB target. Also small GFP-fluorescent axon bundles extend through the lateral half of the pAOB (*large arrow*). In the MOB, the mGC is shifted and less well innervated compared with heterozygous NP2-Δ mice, and the nGl have a more disorganized appearance. *D*, Another example of a homozygous NP2-Δ mouse. The NP2-expressing VSN axonal tracts approach the AOB from a very posterior direction. Also, the mGC has shifted in the opposite direction compared with the previous example. nGl are disorganized or missing. *E–H*, V1rb2-expressing VSN innervation of the aAOB in different NP2 backgrounds as visualized by X-gal staining. A normal innervation pattern of the anterior AOB is seen in wild-type (+/+) and heterozygous (+/−) mice. All axons remain anterior. In homozygous (−/−) mice, V1rb2 axons are misrouted into the pAOB (*G*, *small arrows*) and sometimes form glomerular-like structures (*H*, *small arrows*). Innervation patterns in the anterior AOB are comparable with +/+ and +/− mice. *Red dots* demarcate aAOB from pAOB. Anterior is at *top*; medial to the *right*. Scale bars, 250 μm.

4*B*). These bundles do reach the AOB, although many approach it from abnormal directions (Figs. 4*B*, 5*C,D*).

The most dramatic phenotype is observed in NP2-positive axon innervation of the AOB. Whereas NP2-expressing VSN axons normally only innervate the anterior half of the AOB, axons of NP2-deficient VSNs not only innervate the anterior AOB but also the medial half of the posterior AOB. Quantification reveals that the area covered by tauGFP-positive fibers in the AOB increases by approximately one-half: from 45.1 ± 2.3% (SEM; $n = 6$) in heterozygous mice to 65.4 ± 4.7% ($n = 5$) in homozygous mice. Moreover, apparently lost axons are seen to cross the lateral half of the posterior AOB en route to the anterior AOB (Fig. 5*C,D*). In sections, it is obvious that this inappropriate projection is not confined to the nerve layer alone but extends to the glomerular layer of the posterior AOB (Fig. 6*B*). Because there appears to be massive innervation by NP2-positive axons of glomeruli in the posterior AOB, which is normally occupied by $G_{o\alpha}$-expressing axons, we asked whether these misrouted axons originate from the $G_{i2\alpha}$ layer and examined the fate of the $G_{o\alpha}$-expressing axons from the basal layer of the VNO. Invariably, tauGFP-positive axons also express $G_{i2\alpha}$, even if they innervate the posterior AOB, as is demonstrated by a complete overlap of anti-$G_{i2\alpha}$ antibody labeling and GFP fluorescence in homozygous NP2-Δ mice (Fig. 6*C*). Furthermore, no obvious alteration of the epithelial VNO layers is detected (Fig. 2*G*). Double labeling of the AOB with an anti-$G_{o\alpha}$ antibody shows that there is no double staining between tauGFP-positive axons in the posterior AOB and the endogenous $G_{o\alpha}$-positive axons (Fig. 6*D*). Together, these results indicate that the aberrant innervation of axons of VSNs from the apical layer of the VNO to the glomeruli of the posterior AOB results in a displacement of axons originating from the basal layer of the VNO.

To determine how the loss of NP2 affects target innervation at the level of individual sensory neurons expressing a specific *V1r* gene, we crossed NP2-Δ mice to a mouse strain in which *V1rb2* is tagged with the axonal marker taulacZ (Rodriguez et al., 1999). This allows us to visualize the behavior of V1rb2-expressing VSNs in an NP2 mutant background by relying on the surrogate taulacZ marker. Normally, V1rb2-expressing VSN axons follow the same path to their target region, as is seen with tauGFP axon tracts (Fig. 4*C,D*). They innervate the anterior AOB in variable patterns, as has been described previously (Rodriguez et al., 1999) (Figs. 5*E,F*, 6*E*). In a homozygous NP2-Δ background, axons of V1rb2-expressing VSNs again mirror the behavior observed with NP2-deficient, tauGFP-positive axonal tracts (Fig. 4*B*). Axons of V1rb2-expressing, NP2-deficient OSNs reach the MOB, where they fan out over a greater surface area (Fig. 4*E*) compared with wild-type and NP2-heterozygous backgrounds (Fig. 4*C,D*). Consistent with the general behavior of NP2-deficient VSNs (Fig. 4*B*), axons of V1rb2-expressing, NP2-

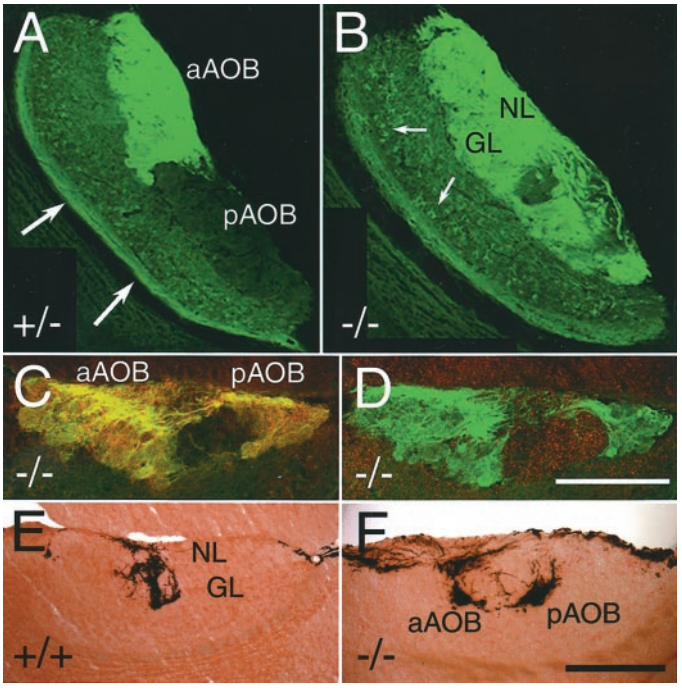

Figure 6. Aberrant sensory innervation of the accessory olfactory bulb: sagittal sections through the AOB. *A*, Sixty micrometer sagittal section through the AOB of a P29 heterozygous NP2-Δ mouse (+/−). VSN axons terminate in the anterior AOB (*aAOB*) and remain clear of the posterior AOB (*pAOB*). Axons of tauGFP-positive mitral and tufted cells are visible at the ventral edge of the AOB (*large arrows*). *B*, Sixty micrometer sagittal section through the AOB of a P29 homozygous NP2-Δ mouse (−/−). Obvious misrouting of tauGFP-positive axons can be seen in the pAOB in addition to normal innervation of the aAOB. Misrouted axons penetrate from the nerve layer (*NL*) into the glomerular layer (*GL*). TauGFP-positive mitral and tufted cell bodies are indicated by *small arrows*. *C*, Twenty micrometer section through the nerve layer and glomerular layer of the AOB of a P35 homozygous NP2-Δ mouse (−/−) stained with an antibody to $G_{i2\alpha}$. There is complete overlap between tauGFP (*green*) and $G_{i2\alpha}$ (*red*) expression, resulting in *yellow*. *D*, Twenty micrometer section through the AOB of a P35 homozygous NP2-Δ mouse stained with an antibody to $G_{o\alpha}$. There is no overlap between tauGFP (*green*) and $G_{o\alpha}$ (*red*) expression. *E*, Innervation of V1rb2-expressing VSNs of the aAOB in an NP2 wild-type (+/+) background, as visualized by X-gal staining. A normal innervation pattern of the anterior AOB is seen. All axons in the NL and glomeruli in the GL remain anterior. *F*, In homozygous (−/−) mice, V1rb2 axons are misrouted to the pAOB where they form glomerular-like structures. Anterior is to the *left*; dorsal is at *top*. Scale bar, 200 μm.

deficient VSNs reach the AOB from many different directions. These atypical approaches of innervation may have routed axons over inappropriate areas, causing them to innervate the posterior AOB (Fig. 5*D,H*). However, even when the axons arrive closer to the midline, they turn posteriorly to innervate the wrong part of the AOB (Fig. 5*C,G*). Interestingly, innervation of the anterior AOB by axons of V1rb2-expressing, NP2-deficient VSNs is similar to that of wild-type or heterozygous mice, although some V1rb2-positive axons form glomerular-like structures in inappropriate areas (Figs 5*H*, *arrows*, 6*F*). It is not clear, however, whether these ectopic structures represent functional glomeruli. The phenotypes described above persist throughout adult life: there appears to be no correction of the pathfinding errors both in the MOB and AOB in mice as old as 4 months.

Sema3 expression in the olfactory bulb

NP2 was first described as a homolog to NP1, which was identified as a coreceptor for the class 3 semaphorin family of secreted axon pathfinding molecules (He and Tessier-Lavigne, 1997; Kolodkin et al., 1997). Subsequently, NP2 was implicated in mediating the repulsive activity of two members of the class 3 semaphorin family, sema3B and sema3F, and together with NP1, a coreceptor for another class 3 semaphorin, sema3C (Chen et al., 1997; Giger et al., 1998; Zou et al., 2000). Sema3F was shown to be moderately expressed in a medial-to-lateral gradient across the MOB during development but was reported to be completely absent in the AOB (Giger et al., 1998).

Because both OSNs and VSNs are continuously renewed and send new axons toward their glomerular targets during all of adult life (Graziadei and Monti Graziadei, 1978), we visualized *sema3B*, *sema3C*, and *sema3F* gene expression in later-stage olfactory bulbs. At postnatal day 21 (P21) and P37, *in situ* hybridization shows expression of *sema3B* (Fig. 7*A*) and *sema3C* (Fig. 7*B*) mostly by mitral cells and the immediately underlying layers of granule cells in the MOB but not anywhere in the AOB (Fig. 7*D*; data not shown). Interestingly, in contrast to sema3F during development (Giger et al., 1998), *sema3B* and *sema3C* signals are uniform across the medial-to-lateral aspects of the MOB (Fig. 7*E*; data not shown). No *sema3F* is detected above the background level in both the MOB and AOB at this stage, by both RT-PCR and *in situ* hybridization (Fig. 7*C*). Together with the continued expression of NP2 in a subset OSNs and VSNs, these results indicate a possible role for these sema3 family members in the observed phenotypes in the MOB both during development and in adult life.

DISCUSSION

Axon guidance to the MOB

The mechanisms whereby OSNs establish a precise map of innervation onto glomerular targets in the MOB are poorly understood (Mombaerts, 2001). The odorant receptors themselves perform a crucial role in guiding sensory axons to the correct site in the bulb (Mombaerts et al., 1996; Wang et al., 1998). OSNs expressing a given OR are located within one of four distinct zones of the olfactory epithelium (Ressler et al., 1993; Vassar et al., 1993). So far, however, only one candidate guidance molecule, the olfactory cell adhesion molecule, OCAM, is expressed in a zonal manner (Yoshihara et al., 1997). Other guidance molecules are expressed in glomeruli that reside in discrete bulbar domains, but these do not correspond directly to the epithelial zones (Nagao et al., 2000). Each glomerulus could potentially be assigned a combinatorial code for its position within the olfactory bulb, with the corresponding OR specifying the final "address" within increasingly broader areas of expression of other guidance molecules.

Among the established guidance molecules expressed in the olfactory system are two coreceptors for class 3 semaphorins, NP1 and NP2. Most efforts to date have been focused on elucidating the role of NP1 in the establishment of OSN connections to the bulb. These efforts have been hampered by embryonic lethality resulting from loss of NP1 function before any olfactory axonal outgrowth (Kitsukawa et al., 1997). The use of a dominant negative NP1 mutation, however, indicates a role for NP1 in preventing premature innervation of OSNs into the early chick telencephalon (Renzi et al., 2000). Removal of the optimal NP1 ligand sema3A results in formation of NP1-positive glomeruli in inappropriate locations (Schwarting et al., 2000). NP1 is not expressed in the VNO or the AOB (He and Tessier-Lavigne, 1997; Kolodkin et al., 1997).

The involvement of NP2 in establishing sensory innervation of

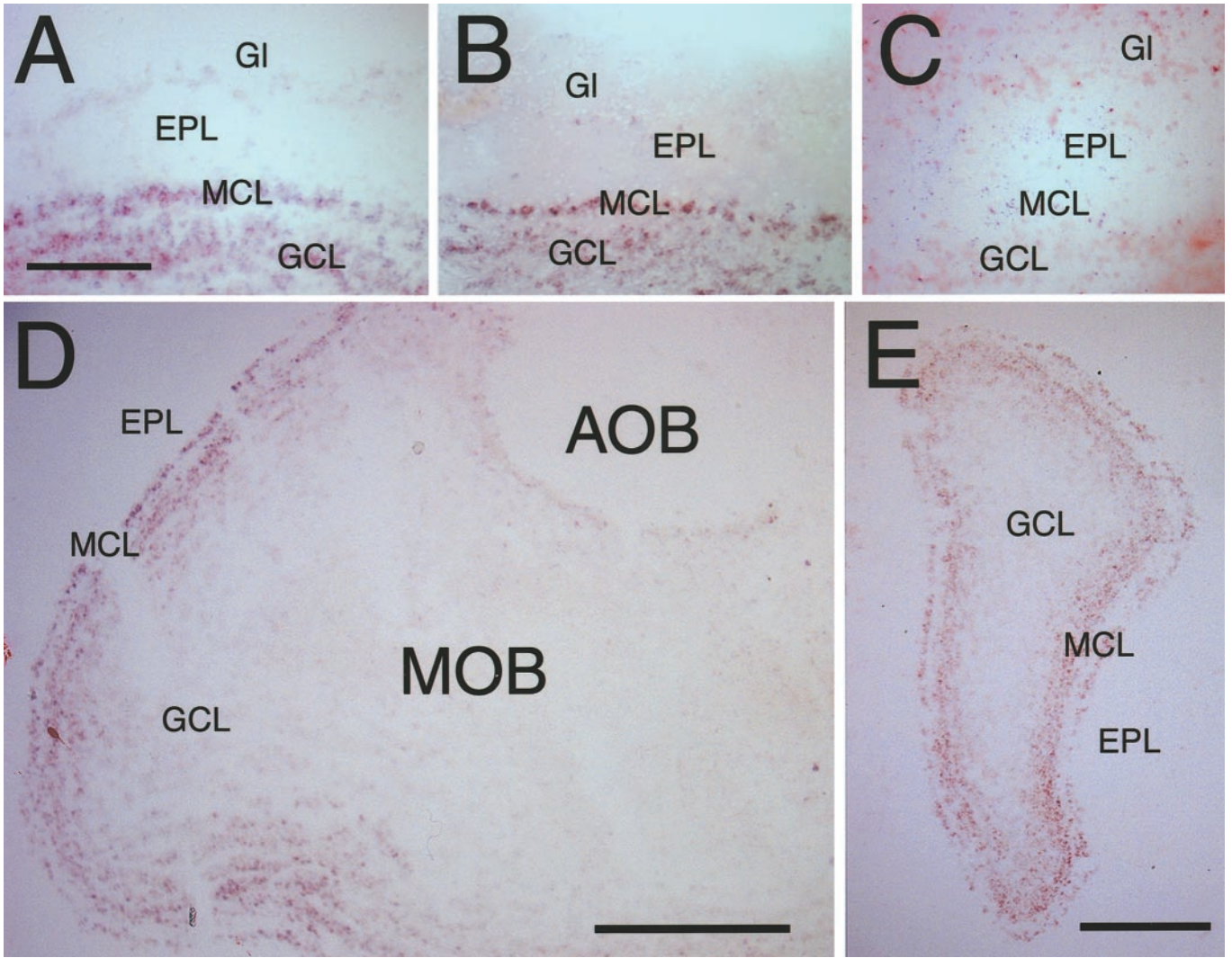

Figure 7. Localization of semaphorins in the olfactory bulb by *in situ* hybridization. *A*, Sagittal section of a P21 olfactory bulb hybridized with a *sema3B* antisense probe. Signal is present in the mitral cell layer (*MCL*) of the MOB and in the subset of granule cells within the granule cell layer (*GCL*) that immediately underlies the MCL. No expression is seen in the external plexiform layer (*EPL*) or within glomeruli (*Gl*). Scale bar, 50 μm. *B*, Sagittal section of a P21 olfactory bulb hybridized with a *sema3C* antisense probe. A similar expression pattern as with *sema3B* is detected. *C*, Sagittal section of a P21 olfactory bulb hybridized with a *sema3F* antisense probe. No signal above background level is observed. *D*, Sagittal section of a P36 olfactory bulb hybridized with a *sema3C* antisense probe. Signal is present in the mitral cell layer (*MCL*) of the MOB and in the subset of granule cells immediately underlying the MCL within the GCL. No expression is seen in and beyond the EPL and anywhere in the AOB. Dorsal is at *top*; anterior to the *left*. Scale bar, 500 μm. *E*, Coronal section of a P36 olfactory bulb hybridized with a *sema3C* antisense probe. Uniform signal is seen within the *MCL* and the outer portion of the GCL. Dorsal is at *top*; medial to the *left*. Scale bar, 250 μm.

the MOB and AOB has not yet been investigated. Of the two previously described NP2 mutations, one completely removes NP2 expression but does not allow visualization of NP2-expressing cells (Giger et al., 2000). The other mutation includes a cellular and axonal marker but leaves ~0.5% of NP2 expression intact, thus creating a severe hypomorph but not a null mutation (Chen et al., 2000). Both studies describe axonal pathfinding errors in multiple CNS areas. Although they both report high expression of NP2 in the olfactory system, analysis of OSN or VSN axonal innervation in NP2 mutant mice has not been presented.

Differential effects of NP2 deficiency on OSN subpopulations

We show that NP2 is expressed in a subset of OSNs projecting to a restricted set of glomeruli mostly in the anterior tip and the ventroposterior region of the MOB. These NP2-positive regions of the MOB overlap but are distinct from the NP1-positive zones described previously (Nagao et al., 2000), hence adding another potential parameter to the combinatorial definition of glomerular positions. The loss of NP2 does not appear to affect grossly this glomerular positioning, with NP2-positive glomeruli still present in the ventroposterior and anterior areas. It will be interesting to determine the effect of the loss of NP2 on OSNs expressing defined, genetically tagged ORs (Mombaerts et al., 1996), but unfortunately, none of the tagged OSN subsets that we can study expresses NP2 (data not shown). Loss of NP2 does affect, however, the ability of individual OSN axons to remain within the glomerular layer. This type of overshooting into the external plexiform layer has been reported to occur on rare occasions during development but not in adult animals (Royal and Key,

1999). Indeed, mature glomeruli appear to trap sensory axons well within their borders, as was demonstrated by prolonged overexpression of GAP43 in OSNs under control of the *OMP* promoter (Holtmaat et al., 1995). These axons targeted their glomeruli but continued to grow inside the glomerulus until they hit the interior border, yet they never overshot into the external plexiform layer (Holtmaat et al., 1995). The expression of three NP2 ligands, sema3B and sema3C continuously and sema3F early on (Giger et al., 1998), in both mitral and granule cells located immediately underneath may explain the reluctance of NP2-expressing OSN axons to penetrate too deeply into the MOB. Indeed, both of these cell types extend their dendrites close to the glomerular layer, ideally suited to release the secreted semaphorins.

One noted exception to the above-described phenotype of overshooting are the necklace glomeruli and the modified glomerular complex. In addition to the obvious distinct glomerular appearance, OSNs projecting to these glomeruli use a different set of signaling molecules (cGMP vs cAMP) for odorant detection (Juilfs et al., 1997) and have been implicated in mediating suckling behavior (Greer et al., 1982). In an NP2-deficient background, both the position and level of innervation of these specialized glomeruli are affected.

Loss of NP2 results in misrouting of vomeronasal axons of the apical layer

VSNs in the two layers of the VNO express two unrelated classes of putative pheromone receptors, or vomeronasal receptors, V1rs and V2rs, and express distinct subunits of G_{α}-protein. NP2 expression is restricted to the apical V1r- and $G_{i2\alpha}$-expressing layer, whereas VSNs in the basal V2r- and $G_{o\alpha}$-expressing layer are NP2-negative. Our results confirm that NP2-positive VSNs from the apical layer innervate the anterior half of the AOB exclusively (Jia and Halpern, 1996). The first phenotype resulting from the loss of NP2 was observed in axons of apical VSNs traversing the medial surface of the MOB. These axons fan out over a larger area and appear generally less directed in their trajectory toward the AOB. It is tempting to speculate that the presence of sema3B and sema3C, and sema3F during development (Giger et al., 1998), in the MOB induces the very directed and fasciculated growth of NP2-positive VSN axons. In fact, mechanisms of how repulsive cues can induce directed growth instead of complete growth cone collapse were demonstrated in other systems before (Fan and Raper, 1995; Zou et al., 2000). A combination of attractive and repulsive cues could induce the formation of tight and directed fascicles across the medial surface of the MOB. $G_{i2\alpha}$-expressing axons eventually reach the AOB in an NP2-mutant background, indicating the presence of NP2-independent cues that attract them to their proper target area.

Once within the AOB, NP2-deficient VSN axons originating from the apical layer display a profound misrouting phenotype, invading the posterior aspect of the AOB. Although the inappropriate innervation pattern can be partially explained by the obscure angles of approach, it is evident that some axons actively turn posteriorly to invade the wrong area of the AOB, yet three established NP2 ligands, sema3B, sema3C, and sema3F, could not be detected in the AOB in this or in previous studies (Chen et al., 1997; Giger et al., 1998, 2000; Chen et al., 2000), ruling out a direct repulsive mechanism for the observed misrouting phenotype. On the other hand, sema3F was shown to be present at high levels in the VNO, indicating a possible cell-autonomous mode of action (Giger et al., 1998). It is not clear, however, how such a mechanism would produce the observed phenotype in the AOB of homozygous NP2-Δ mice. But neuropilin signaling and ligand binding are exceedingly complex; so far, neuropilins have been shown to bind some members of the class 3 semaphorins with varied affinities depending on their partners for dimerization (Chen et al., 1998; Raper, 2000), but not all class 3 semaphorins, some of which are expressed in the olfactory system (Miyazaki et al., 1999), have been investigated. Furthermore, neuropilin binding of one class 3 semaphorin can be modified by other members of the same family (Takahashi et al., 1998), and signal transduction depends on the interaction of the semaphorin–neuropilin complex with yet another class of transmembrane molecules, plexins, adding another level of specificity (Winberg et al., 1998; Takahashi et al., 1999; Tamagnone and Comoglio, 2000). Finally, under certain circumstances, some class 3 semaphorins can act as attractive guidance cues in the olfactory system (de Castro et al., 1999). Interactions between NP1 and the neural cell adhesion molecule L1 have been reported, indicating the possibility of indirect actions of neuropilins on other pathfinding molecules (Castellani et al., 2000). It has also not been ruled out that neuropilins may act as cell adhesion molecules themselves. In this respect, it is interesting to note that a study of the effects of *ephrin5A* mutant mice on the projections of apical sensory neurons to the anterior AOB shows a very similar misrouting phenotype, and that this finding seems to contradict the normal mechanisms proposed for ephrin signaling (Knoll et al., 2001). There is, however, no direct evidence for an interaction between NP2 and ephrinA5 to date. It is thus possible that we have not examined the proper combination of ligands and coreceptors for NP2, and that there may be yet other mechanisms of NP2 activity.

REFERENCES

Castellani V, Chédotal A, Schachner M, Faivre-Sarrailh C, Rougon G (2000) Analysis of the L1-deficient mouse phenotype reveals cross-talk between Sema3A and L1 signaling pathways in axonal guidance. Neuron 27:237–249.

Chen H, Chédotal A, He Z, Goodman CS, Tessier-Lavigne M (1997) Neuropilin-2, a novel member of the neuropilin family, is a high affinity receptor for the semaphorins Sema E and Sema IV but not Sema III. Neuron 19:547–559.

Chen H, He Z, Bagri A, Tessier-Lavigne M (1998) Semaphorin-neuropilin interactions underlying sympathetic axon responses to class III semaphorins. Neuron 21:1283–1290.

Chen H, Bagri A, Zupicich JA, Zou Y, Stoeckli E, Pleasure SJ, Lowenstein DH, Skarnes WC, Chédotal A, Tessier-Lavigne M (2000) Neuropilin-2 regulates the development of selective cranial and sensory nerves and hippocampal mossy fiber projections. Neuron 25:43–56.

de Castro F, Hu L, Drabkin H, Sotelo C, Chédotal A (1999) Chemoattraction and chemorepulsion of olfactory bulb axons by different secreted semaphorins. J Neurosci 19:4428–4436.

Del Punta K, Rothman A, Rodriguez I, Mombaerts P (2000) Sequence diversity and genomic organization of vomeronasal receptor genes in the mouse. Genome Res 10:1958–1967.

Dulac C, Axel R (1995) A novel family of genes encoding putative pheromone receptors in mammals. Cell 83:195–206.

Dymecki S (1996) Flp recombinase promotes site-specific DNA recombination in embryonic stem cells and transgenic mice. Proc Natl Acad Sci USA 93:6191–6196.

Fan J, Raper JA (1995) Localized collapsing cues can steer growth cones without inducing their full collapse. Neuron 14:263–274.

Giger RJ, Urquhart ER, Gillespie SKH, Levengood DV, Ginty DD, Kolodkin AL (1998) Neuropilin-2 is a receptor for semaphorin IV: insight into the structural basis of receptor function and specificity. Neuron 21:1079–1092.

Giger RJ, Cloutier JF, Sahay A, Prinjha RK, Levengood DV, Moore SE, Pickering S, Simmons D, Rastan S, Walsh FS, Kolodkin AL, Ginty DD, Geppert M (2000) Neuropilin-2 is required in vivo for selective axon guidance responses to secreted semaphorins. Neuron 25:29–41.

Graziadei PPC, Monti Graziadei GA (1978) Continuous nerve cell renewal in the olfactory system. In: Development of sensory systems (Jacobsons M, ed), pp 55–83. Berlin: Springer.

Greer CA, Stewart WB, Teicher MH, Shepherd GM (1982) Functional development of the olfactory bulb and a unique glomerular complex in the neonatal rat. J Neurosci 12:1744–1759.
Halpern M (1987) The organization and function of the vomeronasal system. Annu Rev Neurosci 10:325–362.
He Z, Tessier-Lavigne M (1997) Neuropilin is a receptor for the axonal chemorepellent semaphorin III. Cell 90:739–751.
Hirota S, Ito A, Morii E, Wanaka A, Tohyama M, Kitamura Y, Nomura S (1992) Localization of mRNA for c-kit receptor and its ligand in the brain of adult rats: an analysis using in situ hybridization histochemistry. Brain Res Mol Brain Res 15:47–54.
Holtmaat AJ, Dijkhuizen PA, Oestreicher AB, Romijn HJ, Van der Lugt NM, Berns A, Margolis FL, Gispen WH, Verhaagen J (1995) Directed expression of the growth-associated protein B-50/GAP-43 to olfactory neurons in transgenic mice results in changes in axon morphology and extraglomerular fiber growth. J Neurosci 15:7953–7965.
Hooper M, Hardy K, Handyside A, Hunter S, Monk M (1987) HPRT-deficient (Lesch-Nyhan) mouse embryos derived from germline colonization by cultured cells. Nature 326:292–295.
Jia C, Halpern M (1996) Subclasses of vomeronasal receptor neurons: differential expression of G proteins ($G_{\iota\alpha 2}$ and $G_{o\alpha}$) and segregated projections to the AOB. Brain Res 719:117–128.
Juilfs DM, Fülle HJ, Zhao AZ, Houslay MD, Garbers DL, Beavo JA (1997) A subset of olfactory neurons that selectively express cGMP-stimulated phosphodiesterase (PDE2) and guanylyl cyclase-D define a unique olfactory signal transduction pathway. Proc Natl Acad Sci USA 94:3388–3395.
Keverne EB (1999) The vomeronasal organ. Science 286:716–720.
Kitsukawa T, Shimizu M, Sanbo M, Hirata T, Taniguchi M, Bekku Y, Yagi T, Fujisawa H (1997) Neuropilin-semaphorin III/D-mediated chemorepulsive signals play a crucial role in peripheral nerve projection in mice. Neuron 19:995–1005.
Knoll B, Zarbalis K, Wurst W, Drescher U (2001) A role for the EphA family in the topographic targeting of vomeronasal axons. Development 128:895–906.
Kolodkin AL, Levengood DV, Rowe EG, Tai YT, Giger RJ, Ginty DD (1997) Neuropilin is a semaphorin III receptor. Cell 90:753–762.
Lakso M, Pichel JG, Gorman JR, Sauer B, Okamoto Y, Lee E, Alt FW, Westphal H (1996) Efficient in vivo manipulation of mouse genomic sequences at the zygote stage. Proc Natl Acad Sci USA 93:5860–5865.
Meisami E, Bhatnagar KP (1998) Structure and diversity in mammalian AOB. Microsc Res Tech 43:476–499.
Miyazaki N, Furuyama T, Sakai T, Fujioka S, Mori T, Ohoka Y, Takeda N, Kubo T, Inagaki S (1999) Developmental localization of semaphorin H messenger RNA acting as a collapsing factor on sensory axons in the mouse brain. Neuroscience 93:401–408.
Mombaerts P (2001) How smell develops. Nat Neurosci 4:1192–1998.
Mombaerts P, Wang F, Dulac C, Chao SK, Nemes A, Mendelsohn M, Edmondson J, Axel R (1996) Visualizing an olfactory sensory map. Cell 87:675–686.
Nagao H, Yoshihara Y, Mitsui S, Fujisawa H, Mori K (2000) Two mirror-image sensory maps with domain organization in the mouse MOB. NeuroReport 11:3023–3027.
Norlin EM, Alenius M, Gussing F, Hägglund M, Vedin V, Bohm S (2001) Evidence for gradients of gene expression correlating with zonal topography of the olfactory sensory map. Mol Cell Neurosci 18:283–295.
Pasterkamp RJ, Ruitenberg MJ, Verhaagen J (1999) Semaphorins and their receptors in olfactory axon guidance. Cell Mol Biol 45:763–779.
Raper JA (2000) Semaphorins and their receptors in vertebrates and invertebrates. Curr Opin Neurobiol 10:88–94.
Renzi MJ, Wexler TL, Raper JA (2000) Olfactory sensory axons expressing a dominant-negative semaphorin receptor enter the CNS early and overshoot their target. Neuron 28:437–447.
Ressler KJ, Sullivan SL, Buck LB (1993) A zonal organization of odorant receptor gene expression in the olfactory epithelium. Cell 73:597–609.
Ressler KJ, Sullivan SL, Buck LB (1994) Information coding in the olfactory system: evidence for a stereotyped and highly organized epitope map in the olfactory bulb. Cell 79:1245–1255.
Rodriguez I, Feinstein P, Mombaerts P (1999) Variable patterns of axonal projections of sensory neurons in the mouse vomeronasal system. Cell 97:199–208.
Rossignol M, Gagnon ML, Klagsbrun M (2000) Genomic organization of human neuropilin-1 and neuropilin-2 genes: identification and distribution of splice variants and soluble isoforms. Genomics 70:211–222.
Royal SJ, Key B (1999) Development of P2 olfactory glomeruli in P2-internal ribosome entry site-tau-lacZ transgenic mice. J Neurosci 19:9856–9864.
Schwarting GA, Kostek C, Ahmad N, Dibble C, Pays L, Püschel AW (2000) Semaphorin 3A is required for guidance of olfactory axons. J Neurosci 20:7691–7697.
St. John JA, Key B (2001) EphB2 and two of its ligands have dynamic protein expression patterns in the developing olfactory system. Brain Res Dev Brain Res 126:43–56.
Takahashi T, Nakamura F, Jin Z, Kalb RG, Strittmatter SM (1998) Semaphorins A and E act as antagonists of neuropilin-1 and agonists of neuropilin-2 receptors. Nat Neurosci 1:487–493.
Takahashi T, Fournier A, Nakamura F, Wang LH, Murakami Y, Kalb RG, Fujisawa H, Strittmatter SM (1999) Plexin-neuropilin-1 complexes form functional semaphorin-3A receptors. Cell 99:59–69.
Tamagnone L, Comoglio PM (2000) Signalling by semaphorin receptors: cell guidance and beyond. Trends Cell Biol 10:377–383.
Treloar H, Tomasiewicz H, Magnuson T, Key B (1997) The central pathway of primary olfactory axons is abnormal in mice lacking the N-CAM-180 isoform. J Neurobiol 32:643–658.
Vassar R, Ngai J, Axel R (1993) Spatial segregation of odorant receptor expression in the mammalian olfactory epithelium. Cell 74:309–318.
Vassar R, Chao SK, Sitcheran R, Nunez JM, Vosshall LB, Axel R (1994) Topographic organization of sensory projections to the olfactory bulb. Cell 79:981–991.
Wang F, Nemes A, Mendelsohn M, Axel R (1998) Odorant receptors govern the formation of a precise topographic map. Cell 93:47–60.
Winberg ML, Noordermeer JN, Tamagnone L, Comoglio PM, Spriggs MK, Tessier-Lavigne M, Goodman CS (1998) Plexin A is a neuronal semaphorin receptor that controls axon guidance. Cell 95:903–916.
Yoshihara Y, Kawasaki M, Tamada A, Fujita H, Hayashi H, Kagamiyama H, Mori K (1997) OCAM: a new member of the neural cell adhesion molecule family related to zone-to-zone projection of olfactory and vomeronasal axons. J Neurosci 17:5830–5842.
Zou Y, Stoeckli E, Chen H, Tessier-Lavigne M (2000) Squeezing axons out of the gray matter: a role for slit and semaphorin proteins from midline and ventral spinal cord. Cell 102:363–375.